The Tenth Membrane Region of Band 3 Is Initially Exposed to the Luminal Side of the Endoplasmic Reticulum and Then Integrated into a Partially Folded Band 3 Intermediate†

Tomotake Kanki,‡ Masao Sakaguchi,§ Akiko Kitamura,‡ Takashi Sato,‡ Katsuyoshi Mihara,§ and Naotaka Hamasaki*,‡

Department of Clinical Chemistry and Laboratory Medicine and Department of Molecular Biology, Graduate School of Medical Sciences, Kyushu University, Fukuoka 812-8582, Japan

Received August 12, 2002; Revised Manuscript Received September 26, 2002

ABSTRACT: Band 3 is a typical polytopic membrane protein that mediates anion exchange activity [anion exchanger 1 (AE1)]. Although the topology and topogenesis of ∼40 residues just after transmembrane (TM) 9 have been extensively studied, the topogenesis of this region [tenth region (10thR)] has been unclear. Glycosylation sites created in the 10thR were efficiently glycosylated in a cell-free transcription/translation system, whereas the glycosylation efficiencies were quite low in a cultured cell system. When TM12−14 was deleted or when cycloheximide was added to the culture medium, however, the glycosylation efficiency in the cultured cells increased to the same level as in the cell-free system, indicating that TM12 is essential for the sequestration from oligosaccharyl transferase into membrane and that cycloheximide treatment of the cells can mimic the cell-free system by reducing the rate of chain elongation. The glycosylation efficiency in cultured cells also increased with deletion of TM1−3. These results suggest that the 10thR is transiently extruded into the lumen and then inserted into the membrane. Both TM12 and the distant TM1−3 affect the membrane insertion of the 10thR. This indicates that during the folding of the protein, the 10thR is inserted into the membrane after the TM1−12 segments are properly assembled.

Human erythrocyte band 3 [anion exchanger 1 (AE1)] is a typical membrane protein that mediates anion exchange across the cell membrane (*1*). It consists of two distinct functional domains. The N-terminal cytosolic 40 kDa domain associates with peripheral membrane proteins and forms a membrane anchorage site for the cytoskeleton (*2*, *3*), and the C-terminal membrane 55 kDa domain is responsible for anion exchange (*1*).

The membrane topology of band 3 has been extensively studied, and it is generally believed to span the membrane up to 14 times. There is general agreement about the topology of transmembrane (TM)[1] 1 to TM9 (*4*−*10*). But the topology after TM9 is not well established. There is controversy over whether the region of ∼40 residues just after TM9 [tenth region (10thR)] is exposed to the extracellular or cytoplasmic side of the membrane. Fujinaga et al. (*5*) used membrane permeant and impermeant cysteine labeling reagents to determine the topological location of a cysteine residue substituted at various positions in band 3. After expression of the mutant band 3 in cultured cells, they found that the membrane impermeant reagent could modify the cysteine residues substituted for Ser731, Gly742, Ser745, and Ala751 from outside the cells. Popov et al. (*9*) demonstrated that the glycosylation site created by mutating Lys743 to Asn was glycosylated when expressed in a cell-free translation system. These results indicate that this region is on the extracellular side of the cell (or lumenal side of microsomes). On the other hand, Popov et al. (*10*) demonstrated that the Asn743 glycosylation site mutant was not glycosylated when expressed in the cultured cells. This result suggests that this region is not on the luminal side but on the cytoplasmic side of the membrane. Recently, however, Kuma et al. (*7*) clearly demonstrated that the 10thR is in the membrane and Lys743 is exposed to the cytoplasmic side. They used native red blood cells and microsomes from cultured cells overexpressing the membrane domain of band 3 and showed that trypsin was able to cleave band 3 between Lys743 and Ala744 only when the protease was added from the cytoplasmic side.

The tenth region (10thR) between TM9 and TM11 of band 3 has unusual features. This region is not very hydrophobic; the hydrophobicity plot of band 3 is schematically shown in Figure 1A according to Kyte and Doolottle (*11*), and band 3 is easily extruded from the lipid bilayer by alkaline

† This work was supported by grants-in-aid for scientific research from the Ministry of Education, Science, Sports, and Culture of Japan (to N.H., M.S., and K.M.), by a P&P Grant from Kyushu University (to N.H.), by the Magnetic Health Science Foundation of Japan (to N.H.), and by the Human Frontier Science Program and Core Research for Evolutional Science and Technology (to K.M.).

* To whom correspondence should be addressed: Department of Clinical Chemistry and Laboratory Medicine, Graduate School of Medical Sciences, Kyushu University, Fukuoka 812-8582, Japan. E-mail: hamasaki@cclm.med.kyushu-u.ac.jp. Telephone: 81-92-642-5748. Fax: 81-92-642-5772.

‡ Department of Clinical Chemistry and Laboratory Medicine.

§ Department of Molecular Biology.

[1] Abbreviations: 10thR, tenth region; DPP4, dipeptidyl peptidase IV; ER, endoplasmic reticulum; EndoH, endoglycosidase Hf; HA, hemagglutinin; OSTase, oligosaccharyl transferase; RM, rough microsomal membranes; SA-I, type I signal-anchor sequence; SA-II, type II signal-anchor sequence; TM, transmembrane.

10.1021/bi026619q CCC: $22.00
Published on Web 11/01/2002

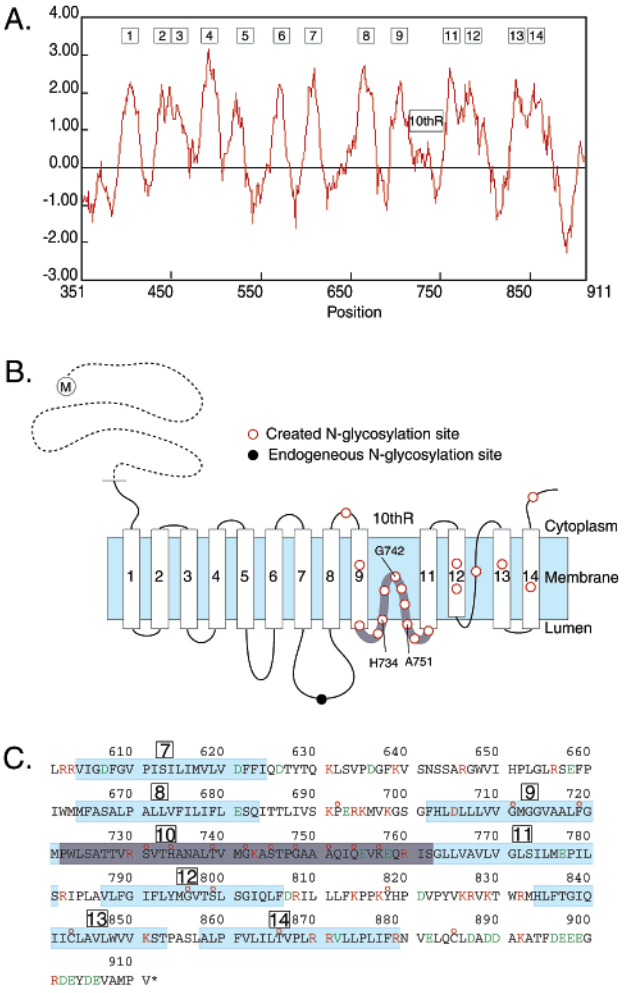

FIGURE 1: (A) Hydrophobicity plots of the membrane domain of band 3 analyzed using the method of Kyte and Doolittle. (B) Topology model of band 3. Band 3 consists of a 40 kDa cytoplasmic domain (···) and a 55 kDa membrane domain (—). The created and endogenous glycosylation sites are denoted with red and black circles, respectively. TM segments are represented by rectangles, and the numbers are shown in the rectangles. (C) Amino acid sequence after TM7 of human band 3. Acidic and basic amino acid residues are denoted with green and red letters, respectively. The positions of the created glycosylation sites are denoted with red circles. The TM segments and 10thR are shown with blue and gray boxes, respectively.

treatment of erythrocyte membranes (*12*), indicating that this region is surrounded by other TM segments in the molecule and not strongly bound to the lipid bilayer (*13*−*15*). This region is thought to include an important site for anion transport (*16*). Studies of the topogenic function of each of the membrane segments of band 3 in the cell-free expression system suggest this region has no topogenic function, so this region alone cannot integrate into the membrane (*6*).

The membrane proteins in the secretory pathway are synthesized by membrane-bound ribosomes; when the signal sequence emerges from the ribosome, it is recognized by the signal recognition particle and the ribosome−nascent polypeptide chain complex is targeted to the endoplasmic reticulum (ER) membrane. The protein is then integrated into the membrane cotranslationally. The translocon is essential for the translocation of the segments facing the extracellular side and for the partition of the transmembrane segments into the lipid bilayer (*17*, *18*). Intrinsic features of hydrophobic sequences determine how they insert into the membrane. Type I and type II signal-anchor sequences (SA-I and SA-II, respectively) form N_{exo}/C_{cyto} and N_{cyto}/C_{exo} orientations, respectively (*19*−*22*), and stop-transfer sequences interrupt translocation (*23*). In multi-membrane-spanning proteins, it has been generally believed that the hydrophobic TM segments are sequentially inserted into the translocon from the amino-terminal side using alternating start-transfer and stop-transfer functions (*24*, *25*). We have studied the topogenesis of band 3 and investigated the topogenic function of each TM segment (*6*). We also found some variations of membrane insertion models. TM2 of band 3 with an insufficient stop-transfer function can be correctly integrated into the membrane only when it is closely apposed to the preceding TM1 (*26*, *27*). TM3 and TM5 with insufficient hydrophobicity for membrane insertion can be integrated into the membrane by a following TM4 and TM6, respectively, with strong SA-I function (*26*, *27*). However, these studies could not explain the topogenesis of the 10thR.

In this study, we have examined the topogenesis of the 10thR using cultured cells and the cell-free expression system and found that the 10thR is transiently exposed to the luminal space to a substantial degree and then inserted into the band 3 molecule from the luminal side. Furthermore, the duration of the exposure is dependent on the translation speed, and the insertion requires other distant TM segments. Our results can explain the disagreement about the topology of the 10thR, especially in the case of Popov et al. (*9*, *10*), by demonstrating the difference in the results obtained from glycosylation studies in the cultured cell system and cell-free translation system. We suggest that during the folding of the protein, the 10thR is only integrated into the rest of the band 3 molecule after TM1−12 have been assembled in the membrane. This process requires extensive interactions with the assembled TM segments which wrap around the 10thR. The unique properties of the 10thR (*6*, *12*−*16*) can be explained by this folding model.

EXPERIMENTAL PROCEDURES

Materials. Enzymes for DNA manipulation and in vitro transcription (Toyobo, Takara, and Promega), endoglycosidase Hf (EndoH, New England Biolabs), antibodies against the HA.11 epitope tag (MMS-101R, Covance), and prestained molecular weight markers (New England Biolabs) were obtained from the indicated sources. Rabbit reticulocyte lysate (*28*) and rough microsomal membranes (RM) from dog pancreas (*29*) were prepared as previously described. RM were washed with 25 mmol of EDTA/L and treated with staphylococcal nuclease (Roche Molecular Biochemicals) to remove endogenous mRNAs as previously described.

DNA Constructs. Each DNA fragment encoding band 3 (Ala352−Val911, Ala352−Ala786, Ala352−Met833, Lys480−Val911, Ile541−Val911, or Asp626−Val911, *Hin*dIII−*Spe*I) was amplified using the appropriate sets of primers. The sense primers contain the *Hin*dIII site, Kozac sequence, and initiator methionine. The antisense primers contain the *Spe*I site. The band 3 fragment (*Hin*dIII−*Spe*I) and the DNA fragment encoding the HA.11 epitope tag (*Xba*I−*Apa*I) were digested with the appropriate restriction enzymes, and were subcloned into a pRcCMV vector (*Hin*dIII−*Apa*I; InvitroGen). For glycosylation scanning mutants, the glycosylation motif (Asn-Ser-Ser) was created

at various positions by point mutation using the method of Kunkel. For TM1−DPP4−14G742N, the SA-II sequence of dipeptidyl peptidase IV (DPP4, Met1−Leu28) was substituted for TM12 (Val787−Lys814) by overlap extension (*30*). Mutants were screened by restriction enzyme mapping and confirmed by sequencing. The sequences of the oligonucleotides that were used are available from the authors upon request.

Analysis Using the Cell-Free Translation System. In vitro transcription and translation were performed essentially as described previously (*31*). Each plasmid was linearized with *Tth*111I and then transcribed with T7 RNA polymerase. The mRNAs were translated in the presence or absence of RM using a cell-free system containing 20% reticulocyte lysate and 15.5 kBq/μL [^{35}S]EXPRESS protein labeling mix (NEN Life Science Products). Salt conditions were optimized as 75 mmol of KOAc/L and 2 mmol of $Mg(OAc)_2$/L. RM were isolated from the translation mixture using a high-salt cushion with ultracentrifugation as previously described and were treated with EndoH (*27*, *32*). After the enzyme reactions were terminated with 10% trichloroacetic acid, the precipitated protein was dissolved in sodium dodecyl sulfate (SDS) sample buffer and analyzed by SDS−PAGE (10% gel). The gel images were visualized using a phosphorimager (FLA2000, Fuji). Quantification was performed using MacBAS software (Fuji).

Analysis Using COS7 Cells. COS7 cells were maintained in Dulbecco's modified Eagle's medium (DMEM) supplemented with 10% fetal calf serum under a 10% CO_2 atmosphere. Transfection of COS7 cells was performed using FuGene reagent (Roche Molecular Biochemicals) essentially as described by Kanaji et al. (*33*). After the cells had been incubated for 20 h, they were used for immunoblotting analysis or pulse-labeling experiments.

For pulse labeling, the culture medium was exchanged with 1 mL of DMEM lacking methionine and cysteine and then incubated for 1 h. Where indicated, cycloheximide was included in the preincubation medium. The cells were labeled with 0.5 mL of DMEM containing 10 μL of [^{35}S]EXPRESS protein labeling mix for 30 min. The cells were scraped with a cell lifter (Costar) into 1 mL of phosphate-buffered saline and pelleted by centrifugation at 5000*g* for 2 min. Then, 50 μL of TSDS [2% SDS and 50 mmol of Tris-HCl/L (pH 7.5)] was added to the cell pellets, and the mixture was briefly sonicated. After 1 mL of dilution buffer [50 mmol of Tris-HCl/L (pH 7.5), 1% Triton X-100, 1% bovine serum albumin, and 1% Trasilol] had been added, the mixture was centrifuged at 12000*g* for 10 min. The anti-HA antibody (1 μL) and a 20% protein A−Sepharose suspension (80 μL) were added to the supernatant, and the mixture was incubated for 1 h at 4 °C. After the resin had been washed four times with washing buffer [0.1% SDS, 1% Triton X-100, 300 mmol of NaCl/L, and 50 mmol of Tris-HCl/L (pH 7.5)], the proteins were solubilized with SDS denaturing buffer and subjected to SDS−PAGE (10% gel). The gel images were visualized by image analysis (FLA2000, Fuji).

For immunoblotting, the cells (on a cultured 10 cm culture dish) were solubilized with 200 μL of SDS denaturing buffer (0.5% SDS and 1% β-mercaptoethanol). The mixture was immediately and briefly sonicated. Where indicated, aliquots were treated with EndoH for 1 h at 37 °C under the buffer conditions recommended by the supplier. Equivalent aliquots were analyzed by SDS−PAGE and subsequent immunoblotting using the anti-HA antibody. Protein bands were visualized with the HRP-labeled anti-rabbit IgG (Biosource) and ECL reagent (Amersham/Pharmacia). Chemiluminescence was detected with LAS1000plus (Fuji).

RESULTS

Topology Model of Band 3 and Experimental Strategy. We examined the exposure of the 10thR in the luminal space by the accessibility to oligosaccharyl transferase (OSTase) in the ER lumen. For this purpose, the cDNA encoding the membrane domain of band 3 (from Ala352 to Val911) fused with the C-terminal tag sequence of hemagglutinin (HA) was subcloned into pRcCMV, expressed in COS7 cells, and also transcribed by T7 RNA polymerase in vitro. We created a potential glycosylation motif (Asn-Ser-Ser) at various positions around the TM9−14 region with two or three point mutations (red circles in Figure 1B,C); e.g., for the TM1−14G742N construct, the Asn-Ser-Ser motif was substituted for the Gly742-Lys743-Ala744 sequence (Figure 2A). The constructs are named according to the position of the potential glycosylation site that was created. These constructs were expressed either in COS7 cells or in a reticulocyte lysate cell-free system supplemented with RM. The glycosylation of the created sites decisively indicates that the sites were exposed in the lumen and accessible to OSTase, the active site of which is separated from the membrane by 12−14 residues (*9*, *34*).

Different Glycosylation Status in the Two Expression Systems. When expressed in COS7 cells and detected by immunoblotting, the wild-type membrane domain (TM1−14wild type) was glycosylated at the endogenous site (black circle in Figure 1B) between TM7 and TM8 (Figure 2B, lane 1). Treatment with endoglycosidase H (EndoH) shifted the upper band down, indicating that the band was glycosylated (Figure 2B, lane 2). The mutant TM1−14G742N, which possesses a glycosylation site at Asn742 in addition to the endogenous site, had two larger bands (Figure 2B, lane 3), both of which disappeared after treatment with EndoH (Figure 2B, lane 4). All the glycosylation site-scanning mutants were expressed in COS7 cells (Figure 2C). The acceptor sites created in the middle of the 10thR (from S731N to G748N) were weakly glycosylated, but other sites were not. To detect the newly synthesized molecule in COS7 cells, we performed a pulse labeling experiment and obtained results that were essentially the same as those of the immunoblotting experiment (Figure 2D).

When expressed in the cell-free system with RM, TM1−14G742N was diglycosylated (Figure 2E, lane 5). EndoH treatment shifted the upper bands down (Figure 2E, lane 6). Essentially the same constructs were diglycosylated in both expression systems (Figure 2C,F). The diglycosylation efficiencies, however, were much higher in the cell-free system than in COS7 cells [Figure 2G; diglycosylation ratios were calculated using the formula (diglycosylation band)/(diglycosylation band + monoglycosylation band)].

These data indicate that the glycosylation sites from H734N to G748N are exposed in the lumen and are accessible to luminal OSTase. According to the 12+14 rule (*9*, *34*), the segment from Pro722 to Ser762 should extend from the membrane; in other words, TM9 ends at Met721

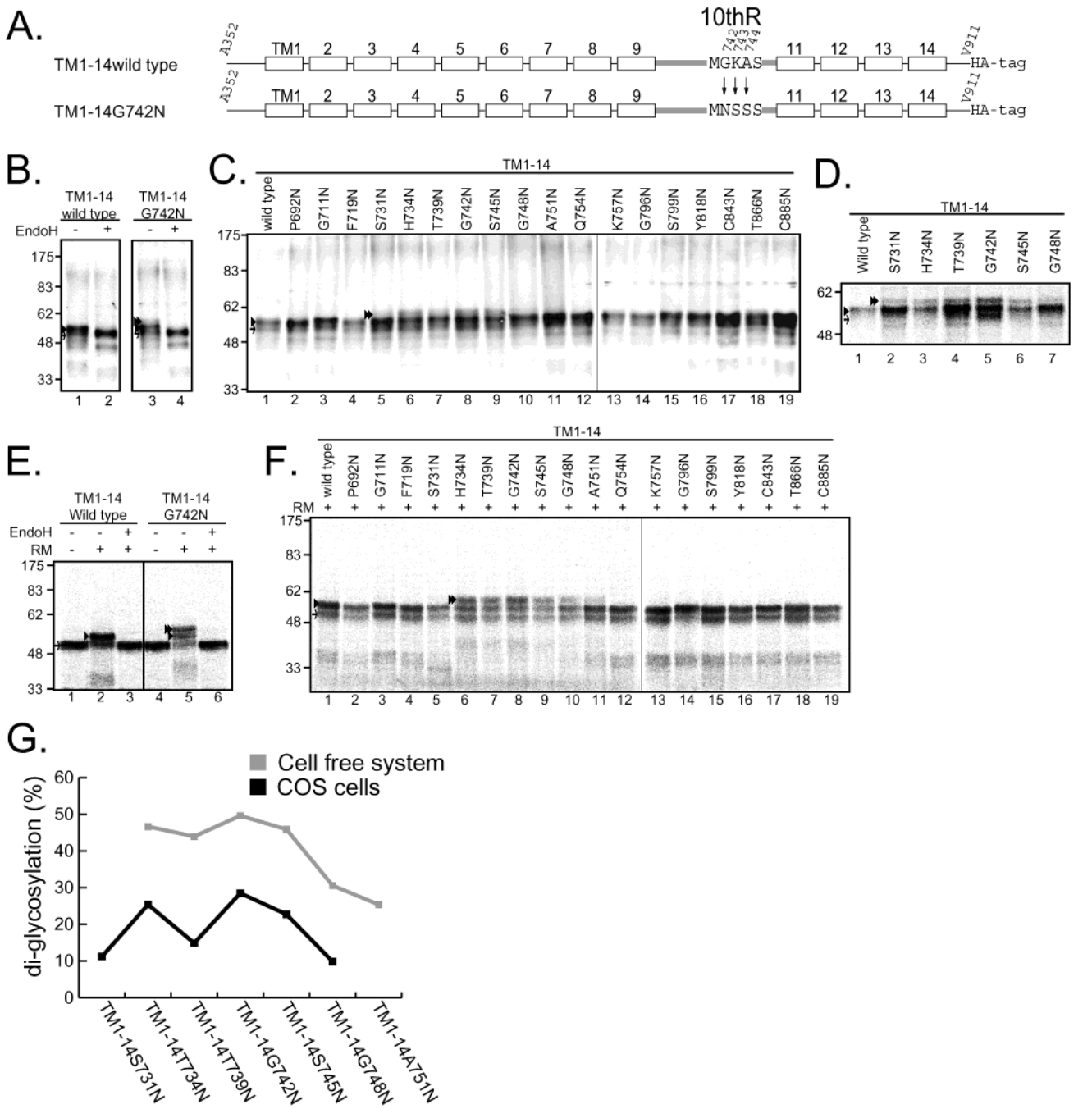

FIGURE 2: Glycosylation state of created sites in COS7 cells and the cell-free system. (A) For the wild-type construct, the membrane domain (from Ala352 to Val911) of band 3 was used (TM1−14wild type). To create a glycosylation motif, the Asn-Ser-Ser motif was substituted for the Gly742-Lys743-Ala744 sequence (TM1−14G742N). (B) Typical results using TM1−14wild type and TM1−14G742N constructs. Constructs were transfected in COS7 cells and incubated for 20 h. Aliquots were treated with (+) or without (−) EndoH and analyzed by SDS−PAGE and subsequently immunoblotted using the anti-HA antibody. The nonglycosylated (arrow), monoglycosylated (arrowhead), and diglycosylated (double arrowheads) forms are indicated. The molecular weight markers are indicated on the left. (C) All of the glycosylation scanning constructs were expressed in COS7 cells, analyzed by SDS−PAGE, and subsequently immunoblotted. (D) The TM1−14 constructs with two possible glycosylation sites were transfected in COS7 cells, pulse labeled for 30 min, and subjected to immunoprecipitation using the anti-HA antibody. (E) Glycosylation in the cell-free system of TM1−14wild type and TM1−14G742N. Both constructs were expressed in the cell-free system in the absence (−) or presence (+) of RM. When expressed in the presence of RM, the membrane vesicles were isolated using a high-salt cushion with ultracentrifugation and then treated with EndoH (+). Samples were analyzed by SDS−PAGE and subsequent image analysis. (F) All TM1−14 constructs were expressed in the cell-free system in the presence of RM and [^{35}S]EXPRESS protein labeling mix and analyzed by SDS−PAGE. Note that almost the same constructs were diglycosylated as in the COS7 cells but the efficiency was increased. (G) Comparison of the glycosylation ratio in the cell-free system and in cultured cells. Diglycosylation ratios were calculated using the formula (diglycosylation band)/(diglycosylation band + monoglycosylation band). Note that the glycosylation ratio in the cell-free system was approximately 2−3 times higher than that in the COS cells.

and TM11 starts at Gly763. The degree of glycosylation, however, was very different between the two expression systems (Figure 2G).

The Following TM Segment Affects the Glycosylation Ratio. We previously demonstrated using red blood cells that the 10thR was extruded from the membrane by trypsin

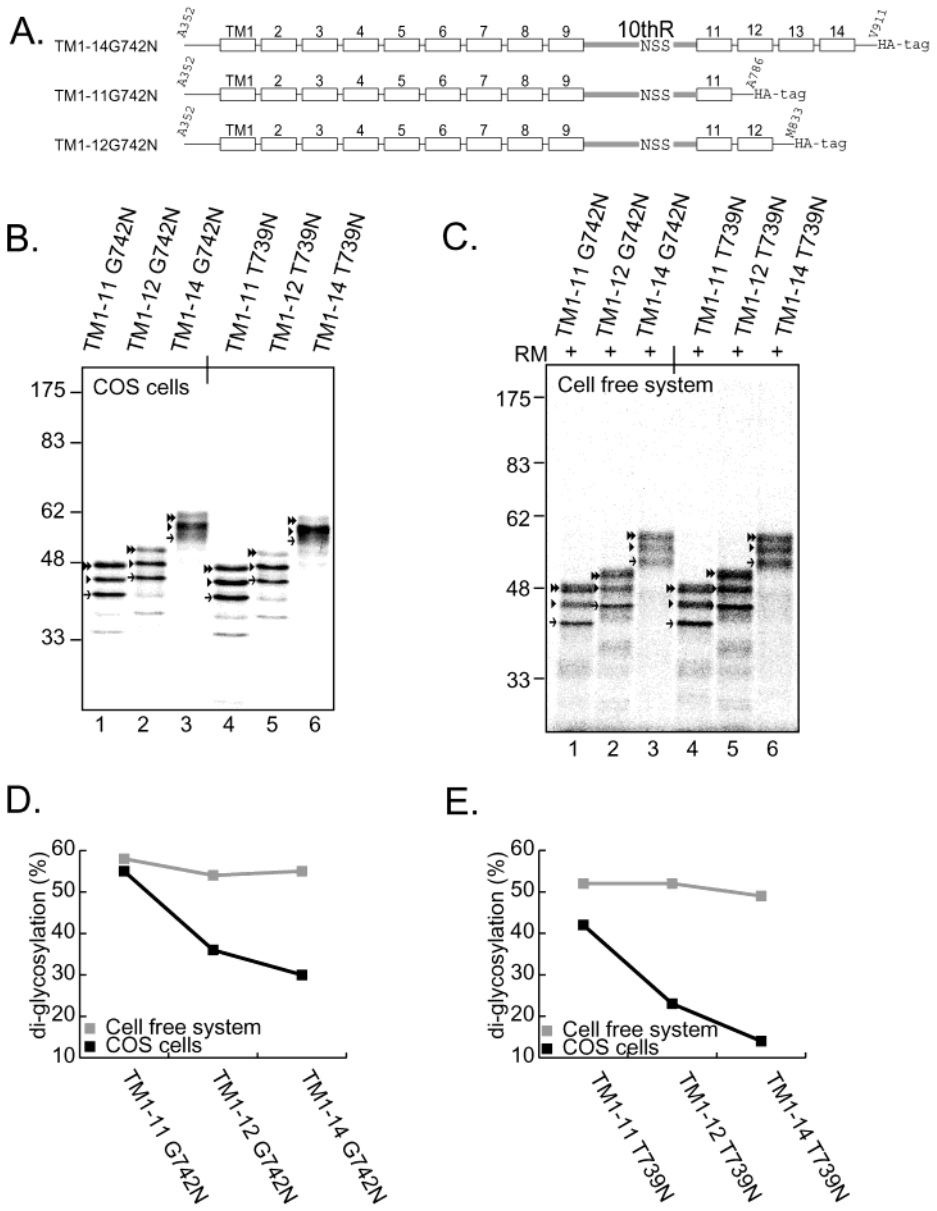

FIGURE 3: TM segments that affected the glycosylation ratio. (A) For the following TM deletion constructs, Val787−Val911 and His834−Val911 were deleted from TM1−14G742N. These were designated according to the created glycosylation site and the included TM segment: TM1−11G742N and TM1−12G742N, respectively. (B) Glycosylation of the C-terminal deletion constructs in COS7 cells. The constructs TM1−11G742N, TM1−12G742N, and TM1−14G742N (lanes 1−3, respectively) were expressed in COS7 cells. The expressed proteins were pulse labeled and immunoprecipitated using the anti-HA antibody. The nonglycosylated (arrow), monoglycosylated (arrowhead), and diglycosylated (double arrowheads) forms are indicated. The same experiments were performed using TM1−11T739N, TM1−12T739N, and TM1−14T739N (lanes 4−6, respectively). (C) Glycosylation of the C-terminal deletion constructs in the cell-free system. The constructs were translated in a cell-free system in the presence of RM and analyzed by SDS−PAGE. The nonglycosylated (arrow), monoglycosylated (arrowhead), and diglycosylated (double arrowheads) forms are indicated. (D) Comparison of the effect of the following TM segment deletions of G742N on the diglycosylation ratio in the cell-free system and in COS7 cells. (E) Comparison of the effect of the following TM segment deletions of T739N on the diglycosylation ratio in the cell-free system and in COS7 cells. Note that the effect of deletion of the following TM segments on the glycosylation ratio tends to be the same when using G742N.

digestion only when the membrane was treated under alkaline conditions. On the other hand, this region was never released from the native red blood cell membrane even after rigorous trypsin digestion (*12*, *13*). These results indicate that the 10thR is surrounded with other TM segments and associated with peptide−peptide interactions (*14*, *15*). We hypothesized that if the TM segments following to the 10thR were deleted, the 10thR would be unable to interact with other TM segments, and the glycosylation sites introduced in this region would be more accessible to OSTase. To examine this possibility, we deleted several TM segments from TM1−14G742N to obtain TM1−11G742N and TM1−12G742N (Figure 3A). In the cell-free system, these constructs were as efficiently diglycosylated as the full-length molecule (Figure 3C, lanes 1−3). In COS7 cells, the deletion of TM12−14 (TM1−11G742N) increased the glycosylation efficiency to a level comparable to that in the cell-free system (Figure 3B, lanes 1−3). Quantification of the bands clearly demonstrated that the glycosylation efficiency in COS7 cells was lowered by the presence of TM12 (Figure 3D). Essentially the same results were obtained with the other glycosylation site mutant (T739N; lanes 4−6 of Figure 3B,

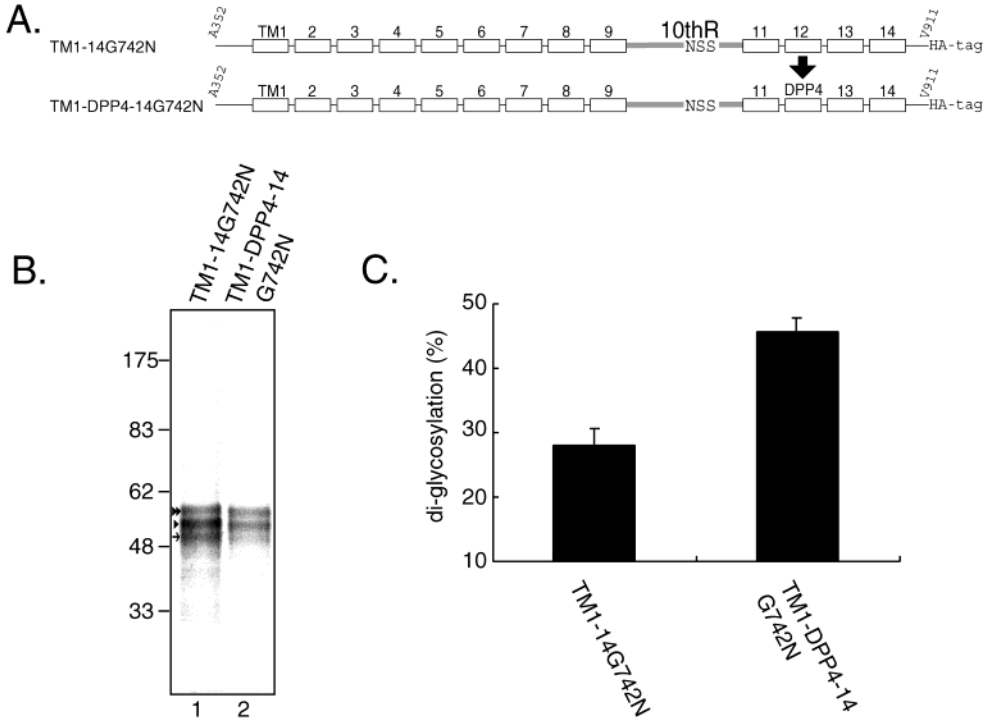

FIGURE 4: Sequestration of the 10thR from OSTase specifically requires the TM12 sequence. (A) For TM1−DPP4−14G742N, the SA-II sequence of DPP4 was substituted for TM12. (B and C) Constructs TM1−14G742N and TM1−DPP4−14G742N were expressed in COS7 cells, pulse labeled, and then analyzed by SDS−PAGE. The glycosylation efficiency increased dramatically when the SA-II segment of DPP4 was substituted for TM12. The data are expressed as the means ± the standard deviation of three independent experiments.

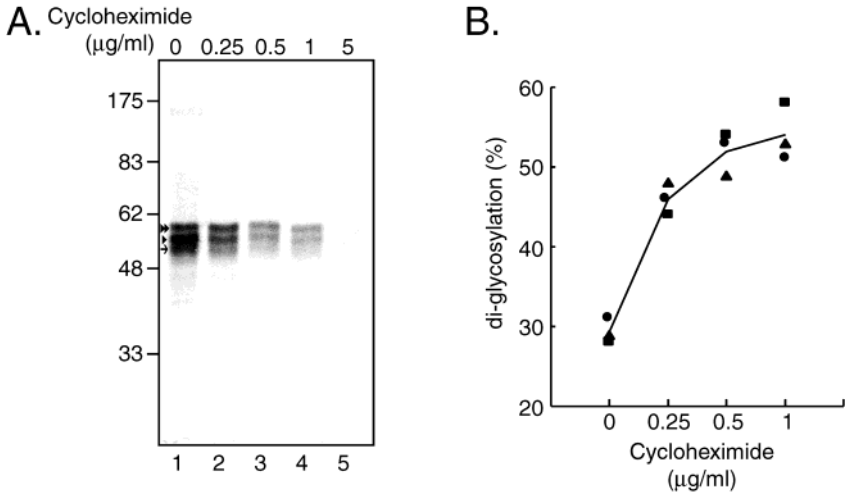

FIGURE 5: Translation rate which affects the exposure of the 10thR to the OSTase. (A) Each concentration of cycloheximide was added 60 min before and during pulse labeling of the TM1−14G742N construct. Samples were subjected to immunoprecipitation using the anti-HA antibody and analyzed by SDS−PAGE. (B) Glycosylation ratios were calculated using the formula (diglycosylation band)/(diglycosylation band + monoglycosylation band). The glycosylation ratio increased on the basis of the dose of cycloheximide. Individual filled points indicate three independent series of experiments, and the solid line indicates the average of the three independent series of experiments.

lanes 4−6 of Figure 3C, and Figure 3E). We concluded that the 10thR is transiently exposed to the luminal space and is then sequestered from the OSTase in a TM12-dependent step. The 10thR is separated from TM12 by TM11, indicating that the effect of TM12 cannot be explained by the topogenic effect of adjacent TM segments as previously reported (*27*).

To examine the specificity of TM12, we exchanged TM12 with the SA-II sequence of DPP4, which has the same N_{cyto}/C_{exo} orientation (*35*) as TM12 (TM1−DPP4−14G742N, Figure 4A). The diglycosylation efficiency of this construct in COS7 cells increased (Figure 4B,C), indicating that sequestration of the 10thR from OSTase specifically requires the TM12 sequence.

The Translation Rate Affects Exposure of the 10thR to the Lumen. In the cell-free system, the 10thR is highly accessible to OSTase despite the presence of TM12 (Figure 3C, lanes 2, 3, 5, and 6). The chain elongation rate in the cell-free system is much slower than in COS7 cells. Thus, there is the possibility that, depending on the delay of TM12 synthesis after exposure of the 10thR to the luminal side, the duration of OSTase access to the 10thR is increased. If this is the case, the rate of protein synthesis should also affect

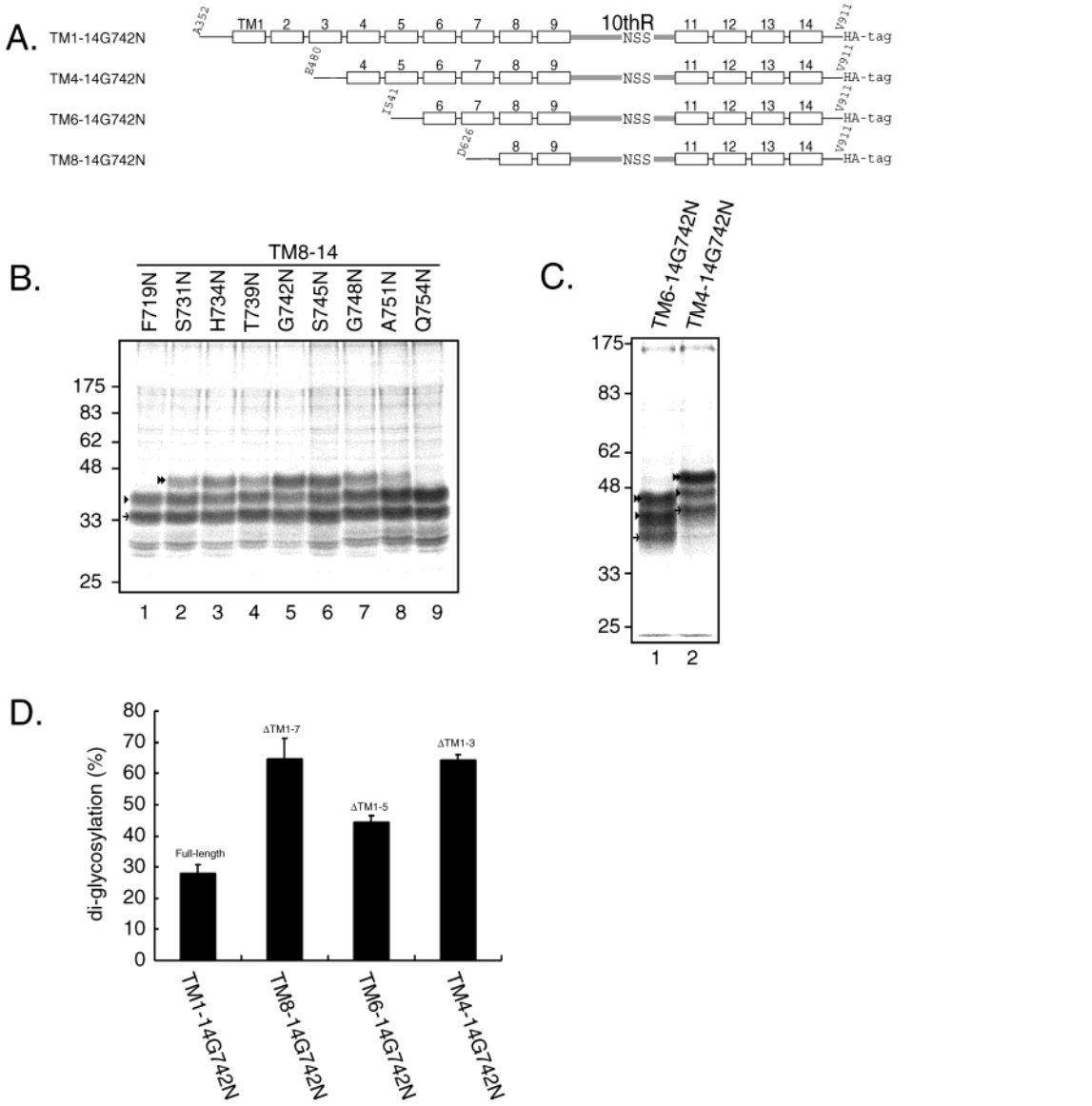

FIGURE 6: Effect of deletions of the preceding TM segments on the glycosylation ratio. (A) For the preceding TM deletion constructs, Ala352−Cys479, Ala352−Leu540, and Ala352−Gln625 were deleted from TM1−14G742N. (B) Glycosylation scanning constructs of TM8−14 were expressed in COS7 cells, pulse labeled, and then analyzed by SDS−PAGE. The nonglycosylated (arrow), monoglycosylated (arrowhead), and diglycosylated (double arrowheads) forms are indicated. (C) Constructs TM6−14G742N and TM4−14G742N were expressed in COS7 cells and pulse labeled. (D) Comparison of the effects of deletion of the preceding TM segments on the glycosylation ratio in COS7 cells. The data are expressed as means ± the standard deviation of three independent experiments. Compared to TM1−14G742N, the deletion of TM1−3, TM1−5, and TM1−7 increased the glycosylation ratio to the same level as in the cell-free experiment (see Figure 2E).

the extent of glycosylation in cultured cells as in the case of the cell-free system. Thus, we examined the effect of cycloheximide, which suppresses the chain elongation rate (*36*, *37*), on the glycosylation ratio. The level of translation products diminished and the relative amount of the diglycosylated form increased, depending on the dose of cycloheximide (Figure 5). This finding indicates that decreasing the chain elongation rate increased the length of the exposure of the 10thR to OSTase and strongly supports the idea that 10thR insertion into the membrane domain depends on the synthesis of TM12.

Deletion of the Preceding TM Segment Affects the Glycosylation Ratio. To examine the effect of other TM segments, we deleted TM1−7 from the series of glycosylation site scanning constructs (TM8−14 versions, Figure 6A). Because TM8 possesses strong SA-I function (*6*), these constructs were expected to be targeted to and correctly inserted into the ER membrane. When expressed in the cell-free system (data not shown) and in COS7 cells (Figure 6B), the same sites were glycosylated as in the case of TM1−14 constructs. The glycosylation efficiencies of these constructs in COS7 cells were much higher than those of the TM1−14 constructs (e.g., compare lanes 2−7 in Figure 2D vs lanes 2−7 in Figure 6B). TM1−5 and TM1−3 were also deleted from TM1−14G742N to make TM6−14G742N and TM4−14G742N, respectively (Figure 6A). These constructs were also glycosylated more efficiently than the TM1−14 construct in COS7 cells (Figure 6C,D). The results indicate that the preceding segments, TM1−3, have critical roles in the sequestration of 10thR. While TM1−3, the 10thR, and TM12 are mutually far apart in the primary amino acid sequence, both TM1−3 and TM12 affect the membrane insertion of

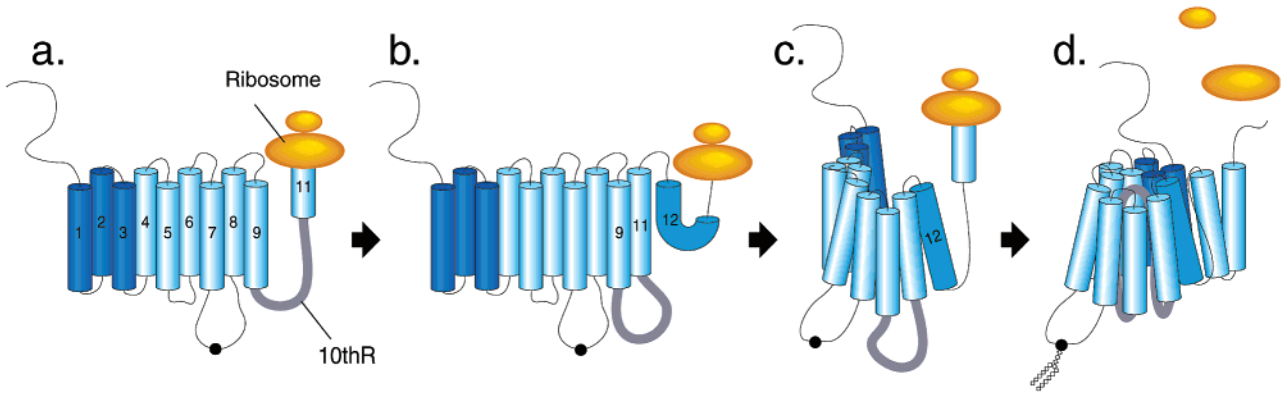

FIGURE 7: 10thR which is initially exposed to the luminal side of the endoplasmic reticulum and acquires its final conformation through a partially folded band 3 intermediate. After TM9 enters the membrane, the 10thR is translocated through the translocon (a). The following TM11 stops the translocation and becomes a transmembrane segment (a to b). At this time, the 10thR is exposed to the lumen and should be accessible to OSTase (b). After TM12 integrates into the membrane, the assembly of TM1−12 in the membrane begins (c). Finally, the 10thR is sequestered into this TM1−12 intermediate from the lumen (d).

the 10thR. This finding strongly suggests that during the folding of the protein, the 10thR is integrated into the band 3 molecule after TM1−12 are assembled in the membrane.

DISCUSSION

In this study, we studied the topogenesis of the 10thR of band 3 by expressing glycosylation constructs in living cells and a cell-free system. Our results indicate that the 10thR was initially transiently exposed to the luminal side of the ER membrane and then inserted into the membrane after the synthesis of TM12. This insertion required not only the following segment (TM12) but also the preceding segments (TM1−3). TM1−3, the 10thR, and TM12 are mutually far apart. Thus, we conclude that the 10thR is incorporated into the band 3 molecule only when TM1−12 of band 3 have been assembled in the membrane as schematically shown in Figure 7d. The duration of 10thR exposure in the ER lumen depends on the folding speed of the whole molecule because the duration of exposure increased when synthesis was carried out in the cell-free translation system or when chain elongation was suppressed with cycloheximide. The requirement of TM12 for the folding of the nascent band 3 is demonstrated by the fact that another hydrophobic segment with the same topogenic function as TM12 (SA-II sequence of DPP4) could not replace TM12 in the efficient sequestration of the 10thR.

Figure 7 shows our proposed model of 10thR insertion. TM9 enters into the membrane by its SA-II function (*6*), and the following 10thR, which has no stop-transfer function (*6*), is translocated through the translocon (Figure 7a). Then the following TM11, which has stop-transfer function (*6*), becomes a TM segment. While TM12 is being synthesized, the 10thR is exposed in the lumen and is accessible to the OSTase active site (Figure 7b), although the duration of this exposure was different in the two expression systems. After TM12 is integrated into the membrane, the assembly of TM1−12 in the membrane begins and a partially folded intermediate is formed (Figure 7c). The presence of this TM1−12 intermediate is required for the 10thR to attain its final structure in the mature band 3 molecule (Figure 7d). This membrane insertion model is novel, because the 10thR is incorporated from the lumenal side into a partially prefolded band 3 molecule which already resides in the ER membrane.

The topology of the 10thR has been controversial, partly because of the different results from glycosylation scanning studies in the cell-free expression system and cultured cells. The glycosylation site mutant Asn743 was well glycosylated when expressed in the cell-free system (*9*), but not glycosylated when expressed in cultured cells (*10*). These results are almost the same as the results shown in this paper (panels C, D, F, and G of Figure 2). Via a detailed study of the topogenesis of the 10thR and demonstrating the increased accessibility of the 10thR to OSTase in living cells using cycloheximide, we can explain the difference in the glycosylation scanning results by the different rates of protein synthesis in the two systems. The topology we propose here (Figure 1B) is compatible with the recent observation that Lys743 was cleaved by trypsin only from the cytoplasmic side using both native red blood cells and ER from cultured cells (*7*).

Wang et al. (*38*) demonstrated that trypsin can cleave wild-type band 3 expressed in the cell-free system between Lys743 and Ala744 from the cytoplasmic side of the ER membrane. This finding indicates that in the cell-free system the final topology of the 10thR of wild-type band 3 is same as the topology in cultured cells and native red blood cells. Furthermore, we reproduced the high accessibility of the 10thR to OSTase in the cultured cells using cycloheximide. These findings that two independent experimental procedures can induce the same effects on glycosylation indicate that the exposure of 10thR in the luminal space occurs in a real folding intermediate of band 3, and is not an artificial conformation produced in only the cell-free system. We suggest that this technique might be useful for investigating the folding mechanisms of other membrane proteins in the ER membrane.

The glycosylation scanning data (panels C, D, and F of Figure 2) clearly indicate that the membrane−lumen boundaries of the two hydrophobic segments, TM9 and TM11, are Met721 and Gly763, respectively (for nomenclature, see Figure 1). Both ends of the 10thR are therefore fixed on the luminal side of the membrane. One of the most striking findings is the clear indication that the efficient sequestration of 10thR strictly requires both the preceding and following TM segments (TM1−3 and TM12, respectively). The insertion mode proposed here is consistent with previous observa-

tions. The transient exposure of 10thR in the luminal space is supported by the fact that this region possesses only limited hydrophobicity (Figure 1A) and possesses no topogenic function (*6*). The 10thR exhibited a prominent peak with high interfacial propensity when we analyzed it according to the interface scale of Wilmley and White (*39*). It suggests that the 10thR has the potential for inserting into the interface of the membrane lipid bilayer. Protein chemical studies on the erythrocyte membrane indicate that the 10thR is extruded by protease treatment only after alkali denaturation (*12*, *14*), supporting the occluded location of the 10thR within the band 3 molecule.

We have studied the topogenesis of band 3 (*6*, *26*, *27*). Via clarification of the insertion mechanism of the 10thR in this work, details of the topogenesis of band 3 can be explained as follows. TM1 mediates ER targeting of the ribosome and starts the translocation of the following segment. TM2 stops translocation only by interacting with the previous TM1 segment. TM3 and TM5 are inserted with the help of the SA-I function of TM4 and TM6, respectively. Although TM7 possesses a start-transfer function, the SA-I function of TM8 contributes to the efficient and correct insertion of the TM7−8 region. TM9 starts the translocation, and TM11 stops it. The 10thR is translocated through the membrane and is inserted into the rest of the molecule after the synthesis of TM12.

It is still unclear how membrane proteins fold. There are two views about this: (i) that transmembrane helices leave the translocon one by one, driven simply by the thermodynamics of lipid partitioning, and then the protein is finally folded; and (ii) that helices initially pack together inside the translocation channel and move out en bloc, in which case the as yet uncharacterized internal environment in the translocation channel might exert a decisive influence on the final structure (*40*). The translocon can accommodate as many as five TM segments in its aqueous environment (*41*). It is unlikely that all of the segments from TM1−3 to TM12 of band 3 can be accommodated within a single translocon, considering the size of the translocons that have been reported recently (*42*−*44*). So in the case of band 3 it is reasonable to suggest that the 10thR is sequestered into the rest of the molecule after almost all of the TM segments are released from the translocon and assembled into a final conformation.

ACKNOWLEDGMENT

We are grateful to Professor Michael J. A. Tanner (Department of Biochemistry, School of Medical Sciences, University of Bristol, Bristol, U.K.) and Dr. Y. Kida (Department of Molecular Biology) for critical comments about the manuscript and useful advice during the experiments.

REFERENCES

1. Passow, H. (1986) *Rev. Physiol. Biochem. Pharmacol. 103*, 61−203.
2. Tanner, M. J. (1993) *Semin. Hematol. 30*, 34−57.
3. Zhang, D., Kiyatkin, A., Bolin, J. T., and Low, P. S. (2000) *Blood 96*, 2925−2933.
4. Tang, X. B., Fujinaga, J., Kopito, R., and Casey, J. R. (1998) *J. Biol. Chem. 273*, 22545−22553.
5. Fujinaga, J., Tang, X. B., and Casey, J. R. (1999) *J. Biol. Chem. 274*, 6626−6633.
6. Ota, K., Sakaguchi, M., Hamasaki, N., and Mihara, K. (1998) *J. Biol. Chem. 273*, 28286−28291.
7. Kuma, H., Shinde, A. A., Howren, T. R., and Jennings, M. L. (2002) *Biochemistry 41*, 3380−3388.
8. Wood, P. G. (1992) *Prog. Cell Res. 2*, 325−352.
9. Popov, M., Tam, L. Y., Li, J., and Reithmeier, R. A. F. (1997) *J. Biol. Chem. 272*, 18325−18332.
10. Popov, M., Li, J., and Reithmeier, R. A. (1999) *Biochem. J. 339*, 269−279.
11. Kyte, J., and Doolittle, R. F. (1982) *J. Mol. Biol. 157*, 105−132.
12. Kang, D., Okubo, K., Hamasaki, N., Kuroda, N., and Shiraki, H. (1992) *J. Biol. Chem. 267*, 19211−19217.
13. Hamasaki, N., Okubo, K., Kuma, H., Kang, D., and Yae, Y. (1997) *J. Biochem. 122*, 577−585.
14. Hamasaki, N., Kuma, H., Ota, K., Sakaguchi, M., and Mihara, K. (1998) *Biochem. Cell Biol. 76*, 729−733.
15. Hamasaki, N., Abe, Y., and Tanner, M. J. (2002) *Biochemistry 41*, 3852−3854.
16. Muller-Berger, S., Karbach, D., Kang, D., Aranibar, N., Wood, P. G., Ruterjans, H., and Passow, H. (1995) *Biochemistry 34*, 9325−9332.
17. Heinrich, S. U., Mothes, W., Brunner, J., and Rapoport, T. A. (2000) *Cell 102*, 233−244.
18. Mothes, W., Heinrich, S. U., Graf, R., Nilsson, I., von Heijne, G., Brunner, J., and Rapoport, T. A. (1997) *Cell 89*, 523−533.
19. Sabatini, D. D., Kreibich, G., Morimoto, T., and Adesnik, M. (1982) *J. Cell Biol. 92*, 1−22.
20. Wickner, W. T., and Lodish, H. F. (1985) *Science 230*, 400−407.
21. Kida, Y., Sakaguchi, M., Fukuda, M., Mikoshiba, K., and Mihara, K. (2000) *J. Cell Biol. 150*, 719−729.
22. Sakaguchi, M., Tomiyoshi, R., Kuroiwa, T., Mihara, K., and Omura, T. (1992) *Proc. Natl. Acad. Sci. U.S.A. 89*, 16−19.
23. Kuroiwa, T., Sakaguchi, M., Mihara, K., and Omura, T. (1991) *J. Biol. Chem. 266*, 9251−9255.
24. Hegde, R. S., and Lingappa, V. R. (1997) *Cell 91*, 575−582.
25. Goder, V., and Spiess, M. (2001) *FEBS Lett. 504*, 87−93.
26. Ota, K., Sakaguchi, M., Hamasaki, N., and Mihara, K. (2000) *J. Biol. Chem. 275*, 29743−29748.
27. Ota, K., Sakaguchi, M., von Heijne, G., Hamasaki, N., and Mihara, K. (1998) *Mol. Cell 2*, 495−503.
28. Jackson, R. J., and Hunt, T. (1983) *Methods Enzymol. 96*, 50−74.
29. Walter, P., and Blobel, G. (1983) *Methods Enzymol. 96*, 682−691.
30. Ho, S. N., Hunt, H. D., Horton, R. M., Pullen, J. K., and Pease, L. R. (1989) *Gene 77*, 51−59.
31. Sakaguchi, M., Hachiya, N., Mihara, K., and Omura, T. (1992) *J. Biochem. 112*, 243−248.
32. Kato, Y., Sakaguchi, M., Mori, Y., Saito, K., Nakamura, T., Bakker, E. P., Sato, Y., Goshima, S., and Uozumi, N. (2001) *Proc. Natl. Acad. Sci. U.S.A. 98*, 6488−6493.
33. Kanaji, S., Iwahashi, J., Kida, Y., Sakaguchi, M., and Mihara, K. (2000) *J. Cell Biol. 151*, 277−288.
34. Nilsson, I. M., and von Heijne, G. (1993) *J. Biol. Chem. 268*, 5798−5801.
35. Ogata, S., Misumi, Y., and Ikehara, Y. (1989) *J. Biol. Chem. 264*, 3596−3601.
36. Ogg, S. C., and Walter, P. (1995) *Cell 81*, 1075−1084.
37. Goder, V., Crottet, P., and Spiess, M. (2000) *EMBO J. 19*, 6704−6712.
38. Wang, L., Groves, J. D., Mawby, W. J., and Tanner, M. J. (1997) *J. Biol. Chem. 272*, 10631−10638.
39. Wimley, W. C., and White, S. H. (1996) *Nat. Struct. Biol. 3*, 842−848.
40. Chin, C., von Heijne, G., and JW, d. G. (2002) *Trends Biochem. Sci. 27*, 231−234.
41. Borel, A. C., and Simon, S. M. (1996) *Cell 85*, 379−389.
42. Hamman, B. D., Chen, J. C., Johnson, E. E., and Johnson, A. E. (1997) *Cell 89*, 535−544.
43. Menetret, J., Neuhof, A., Morgan, D. G., Plath, K., Radermacher, M., Rapoport, T. A., and Akey, C. W. (2000) *Mol. Cell 6*, 1219−1232.
44. Beckmann, R., Spahn, C. M., Eswar, N., Helmers, J., Penczek, P. A., Sali, A., Frank, J., and Blobel, G. (2001) *Cell 107*, 361−372.

BI026619Q